Three-dimensional rotating flow of Jeffrey fluid for Cattaneo-Christov heat flux model

Tasawar Hayat, Sumaira Qayyum, Maria Imtiaz, et al.

View Online   Export Citation   CrossMark

ARTICLES YOU MAY BE INTERESTED IN

Cattaneo-Christov heat flux model for rotating flow and heat transfer of upper-convected Maxwell fluid
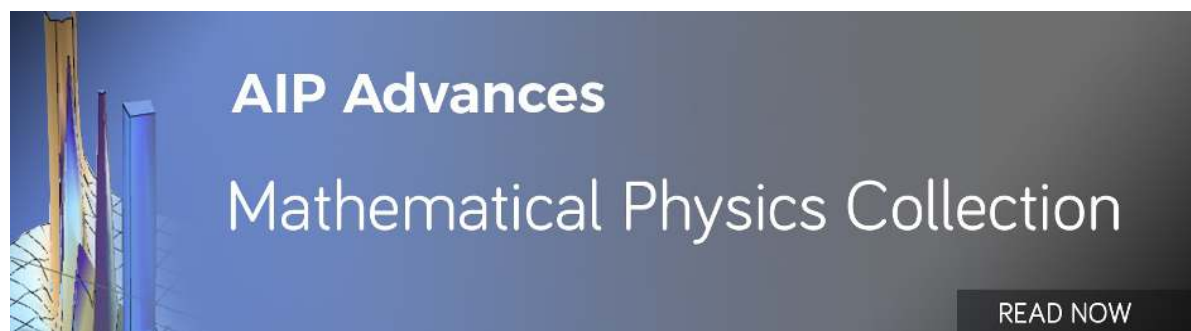AIP Advances **5**, 047109 (2015); https://doi.org/10.1063/1.4917306

Impact of Cattaneo-Christov heat flux in the flow over a stretching sheet with variable thickness
AIP Advances **5**, 087159 (2015); https://doi.org/10.1063/1.4929523

A note on convective heat transfer of an MHD Jeffrey fluid over a stretching sheet
AIP Advances **5**, 117117 (2015); https://doi.org/10.1063/1.4935571

AIP Advances

Mathematical Physics Collection

READ NOW

Three-dimensional rotating flow of Jeffrey fluid for Cattaneo-Christov heat flux model

Tasawar Hayat,[1,2] Sumaira Qayyum,[1] Maria Imtiaz,[1,a] and Ahmed Alsaedi[2]
[1]*Department of Mathematics, Quaid-I-Azam University, 45320, Islamabad 44000, Pakistan*
[2]*Nonlinear Analysis and Applied Mathematics (NAAM) Research Group, Department of Mathematics, Faculty of Science, King Abdulaziz University, Jeddah 21589, Saudi Arabia*

Present study addresses the three dimensional flow of Jeffrey fluid. Flow is induced by a porous stretching sheet. Cattaneo-Christov heat flux model is used to form energy equation. Appropriate transformations are employed to form system of ordinary differential equations. Convergent series solutions are obtained. Impact of pertinent parameters on the velocity and temperature is examined. It is noted that by increasing the ratio of relaxation to retardation times the velocity components are decreased. Temperature distribution also decreases for larger values of thermal relaxation time. © *2016 Author(s). All article content, except where otherwise noted, is licensed under a Creative Commons Attribution (CC BY) license (http://creativecommons.org/licenses/by/4.0/).* [http://dx.doi.org/10.1063/1.4942091]

I. INTRODUCTION

The phenomenon of heat transfer is quite significant in the industrial and biomedical applications e.g. cooling of electronic devices, nuclear reactor cooling, heat conduction in tissues, energy production etc. The mechanism of heat transfer has been successfully described by classical Fourier heat conduction law.[1] Main drawback of this model is that it leads to a parabolic energy equation it means that initial disturbance is immediately sensed by the medium under consideration. This physically unrealistic feature in the literature is referred as "paradox of heat conduction". In order to overcome this enigma, various researchers have proposed alterations in the Fourier's heat conduction law. Cattaneo[2] introduced relaxation time in Fourier law which represents the time required for heat conduction to establish in a volume element when temperature gradient imposed across it. Christov[3] further modified the Cattaneo's model by replacing the ordinary derivative with the Oldroyd's upper convected derivative. Tibullo and Zampoli[4] applied Cattaneo-Christov heat flux model to incompressible fluids. Straughan[5] applied Cattaneo-Christov thermal convection in horizontal layer of incompressible Newtonian fluid under the effect of gravity. Ciarletta and Straughan[6] studied the uniqueness and structural stability Cattaneo-Christov equations. Han *et al.*[7] described the heat transfer and coupled flow of viscoelastic fluid with Cattaneo-Christov heat flux model. Cattaneo-Christov heat flux model is used by Mustafa[8] to discuss the rotating flow of viscoelastic fluid bounded by a stretching sheet.

The study of non-Newtonian fluids has gained interest because of their extensive industrial and technological applications. In view of their differences with Newtonian fluids, several models of non-Newtonian fluids have been proposed. Materials that do not obey the Newtonian law of viscosity are non-Newtonian fluid. Materials like apple sauce, drilling muds, certain oils, ketchup and colloidal and suspension solution are non-Newtonian fluids. The most common and simplest model of non-Newtonian fluids is Jeffrey fluid which has time derivative instead of convected derivative. Tripathi *et al.*[9] studied the peristaltic flow of MHD Jeffrey fluid through a finite length cylindrical tube. Hayat *et al.*[10] discussed the power law heat flux and heat source with radiative

---

[a]Corresponding author Tel.: +925190642172 Email address: mi_qau@yahoo.com

flow of Jeffrey fluid in a porous medium. Turkyilmazolgu[11] analyzed the heat transfer and flow aver a stretching/shrinking surface near the stagnation point. Shehzad *et al.*[12] examined the influences of thermophoresis and Joule heating on the radiative flow of Jeffrey fluid with mixed convection. Das[13] studied the heat transfer and slip effects on peristaltic flow of Jeffrey fluid. Flow of Jeffrey fluid between torsionally oscillating disk is analyzed by Reddy *et al.*[14] Hayat *et al.*[15] investigated the effects of thermal radiation and variable thermal conductivity on Jeffrey fluid flow. Shehzad *et al.*[16] examined the nonlinear thermal radiation in three dimensional flow of Jeffrey nanofluid.

Now a days fluid flow over a stretching surface has gained importance among researchers due to its industrial and engineering processes for example in manufacturing and extraction of polymer and rubber sheets, glass fiber and paper production, manufacture of foods, liquid films in condensation process etc. Crane[17] first of all investigated the stretched sheet flow. Since then various aspects of stretched flow problems have been investigated by several researchers.[18–23] In past most of the work is on the boundary layer flow with stretching surfaces where stretching velocity is directly proportional to the distance from the fixed origin. In such procedures simultaneous heating or cooling and kinematics of stretching have vital impact on the quality of the final product.

In this paper three dimensional flow of Jeffrey fluid is examined by using Cattaneo-Christov heat flux model. The equations are solved analytically by homotopy analysis method (HAM).[24–30] Convergent series solutions are determined. Graphs are plotted and examined for the effects of interesting parameters on the velocity and temperature.

II. MATHEMATICAL FORMULATION

We study the steady three-dimensional incompressible flow of Jeffrey fluid bounded by a porous stretching sheet at $z = 0$. The flow is confined to $z \geq 0$. Fluid rotates about $z-$ axis with angular velocity Ω. The whole system is in a state of rigid body rotation. The sheet is kept at constant temperature T_w whereas T_∞ being ambient temperature such that $T_w \geq T_\infty$. Fluid flow can be expressed by the velocity field $\mathbf{V} = [u(x, y, z), v(x, y, z), W]$. For present problem governing boundary layer equations are as follows:

$$\frac{\partial u}{\partial x} + \frac{\partial v}{\partial y} + \frac{\partial w}{\partial z} = 0, \tag{1}$$

$$u\frac{\partial u}{\partial x} + v\frac{\partial u}{\partial y} + w\frac{\partial u}{\partial z} - 2\Omega v = \frac{\nu}{1 + \lambda_1}\left(\frac{\partial^2 u}{\partial z^2} + \lambda_2\left(\frac{\partial u}{\partial z}\frac{\partial^2 u}{\partial x \partial z} + \frac{\partial v}{\partial z}\frac{\partial^2 u}{\partial y \partial z} + \right.\right.$$
$$\left.\left. \frac{\partial w}{\partial z}\frac{\partial^2 u}{\partial z^2} + u\frac{\partial^3 u}{\partial x \partial z^2} + v\frac{\partial^3 u}{\partial y \partial z^2} + w\frac{\partial^3 u}{\partial z^3}\right)\right), \tag{2}$$

$$u\frac{\partial v}{\partial x} + v\frac{\partial v}{\partial y} + w\frac{\partial v}{\partial z} + 2\Omega u = \frac{\nu}{1 + \lambda_1}\left(\frac{\partial^2 v}{\partial z^2} + \lambda_2\left(\frac{\partial u}{\partial z}\frac{\partial^2 v}{\partial x \partial z} + \frac{\partial v}{\partial z}\frac{\partial^2 v}{\partial y \partial z} + \right.\right.$$
$$\left.\left. \frac{\partial w}{\partial z}\frac{\partial^2 v}{\partial z^2} + u\frac{\partial^3 v}{\partial x \partial z^2} + v\frac{\partial^3 v}{\partial y \partial z^2} + w\frac{\partial^3 v}{\partial z^3}\right)\right), \tag{3}$$

$$\rho c_P\left(u\frac{\partial T}{\partial x} + v\frac{\partial T}{\partial y} + w\frac{\partial T}{\partial z}\right) = -\nabla.\mathbf{q}, \tag{4}$$

where (u, v, w) are the velocities along (x, y, z) direction respectively, ν kinematic viscosity, T the temperature, c_p specific heat, ρ fluid density, λ_1 ratio of relaxation to retardation time, λ_2 retardation time and $\mathbf{q}$ the heat flux satisfying

$$\mathbf{q} + \lambda_3\left(\frac{\partial \mathbf{q}}{\partial t} + \mathbf{V}.\nabla\mathbf{q} - \mathbf{q}.\nabla\mathbf{V} + (\nabla.\mathbf{V})\mathbf{q}\right) = -k\nabla T, \tag{5}$$

in which λ_3 and k are thermal relaxation time and thermal conductivity of fluid respectively. Following Christov,[3] we omit $\mathbf{q}$ by using Eqs. (4) and (5) and obtain

$$u\frac{\partial T}{\partial x} + v\frac{\partial T}{\partial y} + w\frac{\partial T}{\partial z} = \frac{k}{\rho c_p}\frac{\partial^2 T}{\partial z^2} - \lambda_3\left(u^2\frac{\partial^2 T}{\partial x^2} + v^2\frac{\partial^2 T}{\partial y^2} + w^2\frac{\partial^2 T}{\partial z^2} + 2uv\frac{\partial^2 T}{\partial x\partial y} + \right.$$
$$2vw\frac{\partial^2 T}{\partial y\partial z} + 2wu\frac{\partial^2 T}{\partial z\partial x} + \left(u\frac{\partial u}{\partial x} + v\frac{\partial u}{\partial y} + w\frac{\partial u}{\partial z}\right)\frac{\partial T}{\partial x} + \qquad(6)$$
$$\left.\left(u\frac{\partial v}{\partial x} + v\frac{\partial v}{\partial y} + w\frac{\partial v}{\partial z}\right)\frac{\partial T}{\partial y} + \left(u\frac{\partial w}{\partial x} + v\frac{\partial w}{\partial y} + w\frac{\partial w}{\partial z}\right)\frac{\partial T}{\partial z}\right).$$

Corresponding boundary conditions are

$$u = U_w(x) = ax, \ v = V_w(y) = by, \ w = W, T = T_w \ \text{at} \ z \to 0,$$
$$u \to 0, \ v \to 0, \ T \to T_\infty \ \text{when} \ z \to \infty, \qquad(7)$$

where a and b are rates constants having dimension T^{-1}. We consider the following transformations

$$\eta = \sqrt{\frac{a}{\nu}}z, \ u = axf'(\eta), \ v = ayg'(\eta), \ w = -\sqrt{a\nu}(f(\eta) + g(\eta)), \ \theta = \frac{T - T_\infty}{T_w - T_\infty}. \qquad(8)$$

Continuity equation is satisfied automatically and Eqs. (2), (3), and (6) and (7) give

$$f''' + \beta[f''^2 - f'''g' - f''''(f + g)] + (1 + \lambda_1)[f''(f + g) - f'^2 + 2\lambda L^2 g'] = 0, \qquad(9)$$

$$g''' + \beta[g''^2 - g'''f' - g''''(f + g)] + (1 + \lambda_1)[g''(f + g) - g'^2 - 2\lambda/L^2 f'] = 0, \qquad(10)$$

$$\frac{1}{\text{Pr}}\theta'' + (f + g)\theta' - \gamma[(f + g)^2\theta'' + (f + g)(f' + g')\theta'] = 0, \qquad(11)$$

$$f'(0) = 1, f'(\infty) \to 0, f(0) = S,$$
$$g'(0) = \alpha, g'(\infty) \to 0, g(0) = 0, \qquad(12)$$
$$\theta(0) = 1, \theta(\infty) \to 0,$$

where $\lambda = \Omega/a$ denotes the rotation parameter, $\beta = \lambda_2 a$ the Deborah number, $\text{Pr} = \rho c_p \nu/k$ the Prandtl number, $\alpha = b/a$ the ratio of stretching rates, $\gamma = \lambda_3 a$ the thermal relaxation time and $S = -W/\sqrt{a\nu}$ the suction/injection parameter.

III. HOMOTOPIC SOLUTIONS

A. Zeroth-order deformation equations

Initial guesses and auxiliary linear operators are taken as follows:

$$f_0(\eta) = 1 - \exp(-\eta) + S, \ g_0(\eta) = \alpha(1 - \exp(-\eta)), \ \theta_0(\eta) = \exp(-\eta), \qquad(13)$$
$$\mathbf{L}_f = f''' - f', \ \mathbf{L}_g = g''' - g', \ \mathbf{L}_\theta = \theta'' - \theta, \qquad(14)$$

with

$$\mathbf{L}_f\left[c_1 + c_2 e^\eta + c_3 e^{-\eta}\right] = 0,$$
$$\mathbf{L}_g\left[c_4 + c_5 e^\eta + c_6 e^{-\eta}\right] = 0, \qquad(15)$$
$$\mathbf{L}_\theta\left[c_7 e^\eta + c_8 e^{-\eta}\right] = 0,$$

in which $c_i(i = 1 - 8)$ are the constants.

If $q \in [0, 1]$ indicates the embedding parameter and $\hbar_f, \hbar_g$ and $\hbar_\theta$ the non-zero auxiliary parameters then the zeroth order deformation equations are established as follows:

$$(1 - q)\mathbf{L}_f\left[F(\eta, q) - f_0(\eta)\right] = q\hbar_f\mathbf{N}_f[F(\eta, q), G(\eta, q)], \qquad(16)$$

$$(1 - q)\mathbf{L}_g\left[G(\eta, q) - g_0(\eta)\right] = q\hbar_g\mathbf{N}_g[G(\eta, q), F(\eta, q)], \qquad(17)$$

$$(1 - q)\mathbf{L}_\theta\left[\vartheta(\eta, q) - \theta_0(\eta)\right] = q\hbar_\theta\mathbf{N}_\theta[\vartheta(\eta, q), F(\eta, q), G(\eta, q)], \qquad(18)$$

$$F(0, q) = S, \ F'(0, q) = 1, \ F'(\infty, q) = 0, \tag{19}$$

$$G(0, q) = 0, \ G'(0, q) = \alpha, \ G'(\infty, q) = 0, \tag{20}$$

$$\vartheta(0, q) = 1, \vartheta(\infty, q) = 0, \tag{21}$$

where $\mathbf{N}_f, \mathbf{N}_g$ and $\mathbf{N}_\theta$ are given by

$$
\begin{aligned}
\mathbf{N}_f\left[F(\eta, q), G(\eta, q)\right] = {} & \frac{\partial^3 F(\eta, q)}{\partial \eta^3} + \beta\left(\left(\frac{\partial^2 F(\eta, q)}{\partial \eta^2}\right)^2 - \frac{\partial^3 F(\eta, q)}{\partial \eta^3}\frac{\partial G(\eta, q)}{\partial \eta}\right. \\
& \left. - \frac{\partial^4 F(\eta, q)}{\partial \eta^4}(F(\eta, q) + G(\eta, q))\right) + (1 + \lambda_1)\left(\frac{\partial^2 F(\eta, q)}{\partial \eta^2}(F(\eta, q)\right. \\
& \left. + G(\eta, q)) - \left(\frac{\partial F(\eta, q)}{\partial \eta}\right)^2 + 2\lambda L^2\frac{\partial G(\eta, q)}{\partial \eta}\right),
\end{aligned}
\tag{22}
$$

$$
\begin{aligned}
\mathbf{N}_g\left[G(\eta, q), F(\eta, q)\right] = {} & \frac{\partial^3 G(\eta, q)}{\partial \eta^3} + \beta\left(\left(\frac{\partial^2 G(\eta, q)}{\partial \eta^2}\right)^2 - \frac{\partial^3 G(\eta, q)}{\partial \eta^3}\frac{\partial F(\eta, q)}{\partial \eta}\right. \\
& \left. - \frac{\partial^4 G(\eta, q)}{\partial \eta^4}(F(\eta, q) + G(\eta, q))\right) + (1 + \lambda_1)\left(\frac{\partial^2 G(\eta, q)}{\partial \eta^2}(G(\eta, q)\right. \\
& \left. + F(\eta, q)) - \left(\frac{\partial G(\eta, q)}{\partial \eta}\right)^2 - 2\frac{\lambda}{L^2}\frac{\partial F(\eta, q)}{\partial \eta}\right),
\end{aligned}
\tag{23}
$$

$$
\begin{aligned}
\mathbf{N}_\theta\left[\vartheta(\eta, q), F(\eta, q), G(\eta, q)\right] = {} & \frac{1}{\Pr}\frac{\partial^2 \vartheta(\eta, q)}{\partial \eta^2} + (F(\eta, q) + G(\eta, q))\frac{\partial \vartheta(\eta, q)}{\partial \eta} \\
& - \gamma\left((F(\eta, q) + G(\eta, q))^2\frac{\partial^2 \vartheta(\eta, q)}{\partial \eta^2} + (F(\eta, q)\right. \\
& \left. + G(\eta, q))\left(\frac{\partial F(\eta, q)}{\partial \eta} + \frac{\partial G(\eta, q)}{\partial \eta}\right)\frac{\partial \vartheta(\eta, q)}{\partial \eta}\right).
\end{aligned}
\tag{24}
$$

B. mth-order deformation equations

The mth order deformation equations can be written as follows:

$$\mathbf{L}_f\left[f_m(\eta) - \chi_m f_{m-1}(\eta)\right] = \hbar_f \mathbf{R}_{f, m}(\eta), \tag{25}$$

$$\mathbf{L}_g\left[g_m(\eta) - \chi_m g_{m-1}(\eta)\right] = \hbar_g \mathbf{R}_{g, m}(\eta), \tag{26}$$

$$\mathbf{L}_\theta\left[\theta_m(\eta) - \chi_m \theta_{m-1}(\eta)\right] = \hbar_\theta \mathbf{R}_{\theta, m}(\eta), \tag{27}$$

$$f_m(0) = \frac{\partial f_m(0)}{\partial \eta} = \frac{\partial f_m(\infty)}{\partial \eta} = g_m(0) = \frac{\partial g_m(0)}{\partial \eta} = \frac{\partial g_m(\infty)}{\partial \eta} = \theta(0) = \theta(\infty) = 0, \tag{28}$$

where the functions $\mathbf{R}_{f, m}(\eta), \mathbf{R}_{g, m}(\eta)$ and $\mathbf{R}_{\theta, m}(\eta)$ have the following forms

$$
\begin{aligned}
\mathbf{R}_{f, m}(\eta) = {} & f'''_{m-1} + \beta \sum_{k=0}^{m-1}[f''_{m-1-k}f''_k - f''''_{m-1-k}f_k - f''''_{m-1-k}g_k - f'''_{m-1-k}g'_k] \\
& + (1 + \lambda_1)\left(\sum_{k=0}^{m-1}[f_{m-1-k}f''_k + g_{m-1-k}f''_k - f'_{m-1-k}f'_k] + 2\lambda L^2 g'_{m-1}\right),
\end{aligned}
\tag{29}
$$

$$
\begin{aligned}
\mathbf{R}_{g, m}(\eta) = {} & g'''_{m-1} + \beta \sum_{k=0}^{m-1}[g''_{m-1-k}g''_k - g''''_{m-1-k}g_k - g''''_{m-1-k}f_k - g'''_{m-1-k}f'_k] \\
& + (1 + \lambda_1)\left(\sum_{k=0}^{m-1}[g_{m-1-k}g''_k + f_{m-1-k}g''_k - g'_{m-1-k}g'_k] - 2\frac{\lambda}{L^2}f'_{m-1}\right),
\end{aligned}
\tag{30}
$$

$$\mathbf{R}_{\theta,\,m}(\eta) = \frac{1}{\Pr}\theta''_{m-1} + \sum_{k=0}^{m-1}[f_{m-1-k}\theta'_k + g_{m-1-k}\theta'_k] - \gamma\left[f_{m-1-l}\sum_{j=0}^{l}f_{l-j}\theta''_j + g_{m-1-l}\sum_{j=0}^{l}g_{l-j}\theta''_j\right.$$

$$+2f_{m-1-l}\sum_{j=0}^{l}g_{l-j}\theta''_j + f_{m-1-l}\sum_{j=0}^{l}f'_{l-j}\theta'_j + f_{m-1-l}\sum_{j=0}^{l}g'_{l-j}\theta'_j + g_{m-1-l}\sum_{j=0}^{l}f'_{l-j}\theta'_j \qquad (31)$$

$$\left.+g_{m-1-l}\sum_{j=0}^{l}g'_{l-j}\theta'_j\right],$$

$$\chi_m = \begin{cases} 0, & m \le 1 \\ 1, & m > 1 \end{cases}. \qquad (32)$$

The general solutions (f_m, g_m, θ_m) comprising the special solutions $(f_m^*, g_m^*, \theta_m^*)$ are

$$f_m(\eta) = f_m^*(\eta) + c_1 + c_2 e^{\eta} + c_3 e^{-\eta}, \qquad (33)$$

$$g_m(\eta) = g_m^*(\eta) + c_4 + c_5 e^{\eta} + c_6 e^{-\eta}, \qquad (34)$$

$$\theta_m(\eta) = \theta_m^*(\eta) + c_7 e^{\eta} + c_8 e^{-\eta}, \qquad (35)$$

where the constants $c_i(i = 1 - 8)$ through the boundary conditions (28) have the values

$$c_1 = -c_3 - f_m^*(0), \; c_3 = \frac{\partial f_m^*(0)}{\partial \eta}, \; c_4 = -c_6 - g_m^*(0),$$
$$c_6 = \frac{\partial g_m^*(0)}{\partial \eta}, \; c_8 = -\theta_m^*(0), \; c_2 = c_5 = c_7 = 0. \qquad (36)$$

IV. CONVERGENCE ANALYSIS

Homotopy analysis method (HAM) is a powerful technique to solve linear and non-linear problems. HAM involves embedding auxiliary parameters which give the freedom to adjust and control the convergence regions. The auxiliary parameters $\hbar_f, \hbar_g$ and $\hbar_\theta$ have vital role for convergence of series solutions. We plotted $\hbar -$ curves at 10th order of approximations (see Fig. 1a, 1b). Admissible values of auxiliary parameters here are $-0.8 \le \hbar_f \le -0.4, -1.1 \le \hbar_g \le -0.7, \quad -1 \le \hbar_\theta \le -0.5$. Also the HAM solutions converge in the whole region of $\eta(0 \le \eta \le \infty)$ where $\hbar_f = -0.4, \hbar_g = -0.7$ and $\hbar_\theta = -0.5$.

Table I demonstrate the convergence of velocities along the $x-$ and $y-$ directions and temperature. Presented values shows that 15th order of approximations are sufficient for $f''(0)$ and $\theta'(0)$ and 16th order of approximations are enough for the convergence of $g''(0)$.

V. RESULTS AND DISCUSSION

A. Dimensionless velocity profiles

Figs. 2 − 6 show the behavior of ratio of relaxation to retardation times λ_1, Deborah number β, rotational parameter λ, stretching rates ratio α and suction/injection parameter S on both the $x-$ and $y-$ components of velocity f' and g'. Effects of λ_1 on velocities $f'(\eta)$ and $g'(\eta)$ are depicted in Fig. 2. We observed that for increasing λ_1 velocity is decreasing in both directions. An increase in λ_1 corresponds to increase in relaxation time it means particle needs much more time to come back from perturbed system to equilibrium system consequently fluid velocity decreases. Fig. 3 presents the impact of β on the $x-$ and $y-$ component of velocity. The velocity profiles $f'(\eta)$ and $g'(\eta)$ and related momentum boundary layer thicknesses increase for larger Deborah number β because increase in retardation time enhances elasticity. Since elasticity and viscosity are inversely proportional to each other so decrease in viscosity consequently enhances the fluid velocity. Fig. 4
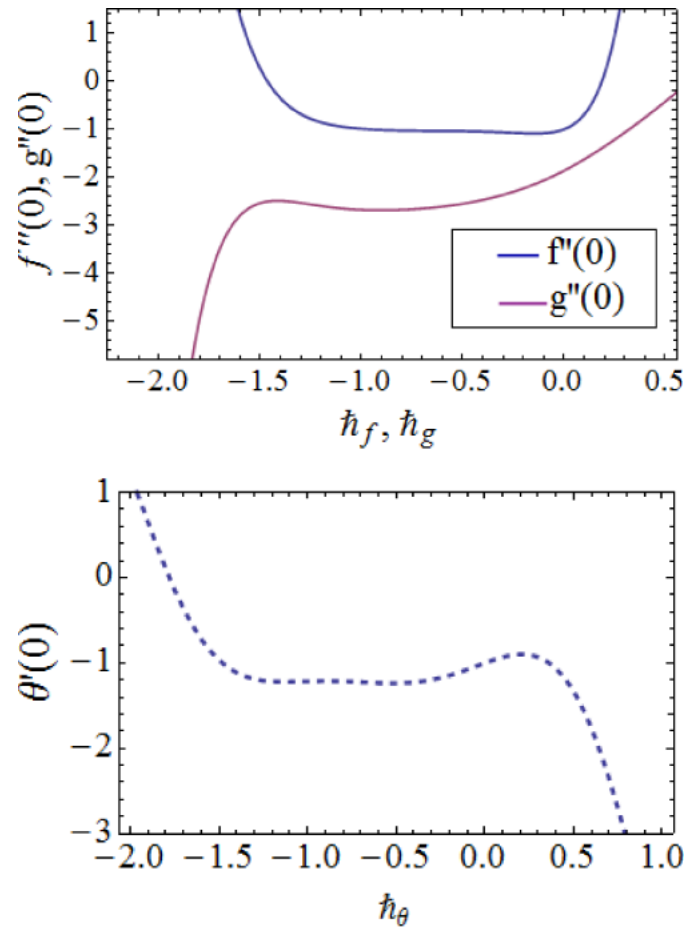
FIG. 1. $\hbar$ − curves for $f''(0), g''(0)$ and $\theta'(0)$ when $\lambda_1 = 0.3, \mathrm{Pr} = 1.4, \beta = 0.5, \lambda = 0.01, \gamma = 0.1, L = \alpha = S = 0.4$.

displays the behavior of velocity profiles for increasing rotation parameter λ. As the rotation parameter increases, the velocity profile along the $x-$ direction increases while the velocity profile along the $y-$ direction decreases. This is because the rotation parameter represents the Coriolis force which leads to accelerate the fluid motion. Fig. 5 shows the impact of stretching rates ratio on the velocity profiles f' and g'. Increasing values of α indicates that rate of stretching is increasing along $y-$ direction so that velocity profile g' is increasing and f' shows decreasing behavior. Influence of suction/injection parameter S on f' and g' is displayed in Fig. 6. Since suction leads to draw the amount of fluid particles therefore the velocity fields f' and g' are decreased.

TABLE I. Convergence of solutions when $\mathrm{Pr} = 1.4, \lambda_1 = 0.3, \beta = 0.5, \lambda = 0.01, \gamma = 0.1$ and $L = \alpha = S = 0.4$.

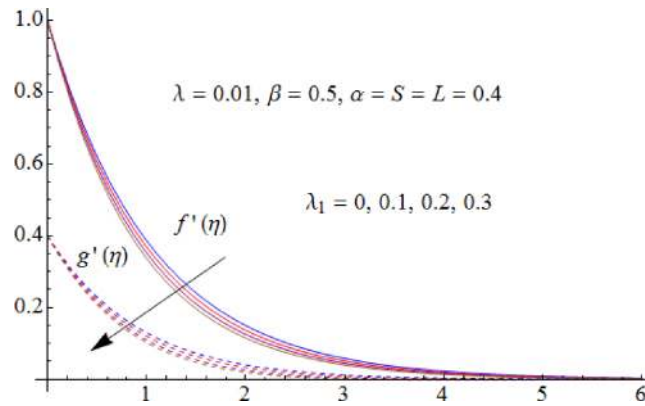| Order of approximation	$-f''(0)$	$-g''(0)$	$-\theta'(0)$
1	1.0720	0.6445	1.0340
5	1.0570	1.4740	1.1440
10	1.0320	2.0070	1.1970
14	1.0330	2.1710	1.2080
15	1.0320	2.1890	1.2090
16	1.0320	2.1980	1.2090
18	1.0320	2.1980	1.2090
20	1.0320	2.1980	1.2090

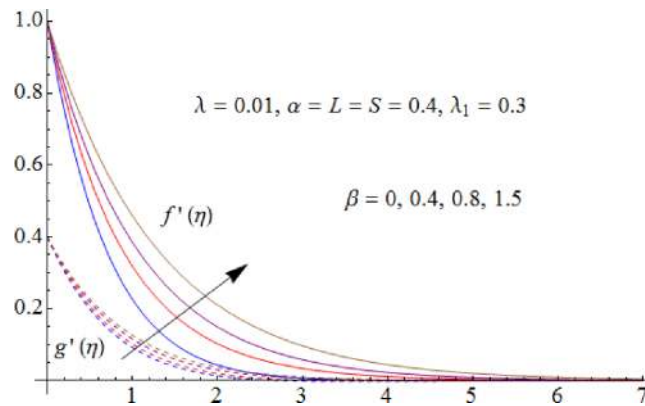FIG. 2. Behavior of λ_1 on $f'(\eta)$ and $g'(\eta)$.

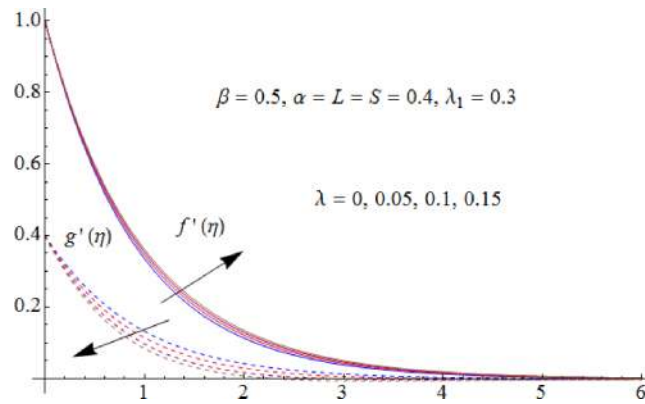FIG. 3. Behavior of β on $f'(\eta)$ and $g'(\eta)$.

FIG. 4. Behavior of λ on $f'(\eta)$ and $g'(\eta)$.

B. Dimensionless temperature profiles

Figs. 7–11 show the behavior of Prandtl number Pr, thermal relaxation time γ, stretching rates ratio α, rotational parameter λ and ratio of relaxation to retardation times λ_1 on temperature profile $\theta(\eta)$. Fig. 7 shows the temperature profile for increasing Prandtl number Pr. For increasing Prandtl number Pr thermal diffusivity decreases so temperature profile decays. Influence of thermal
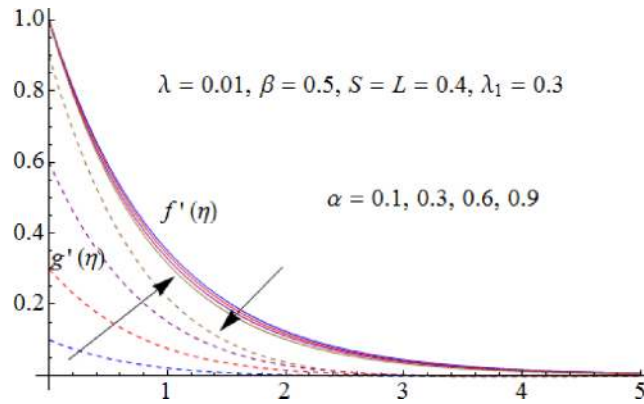
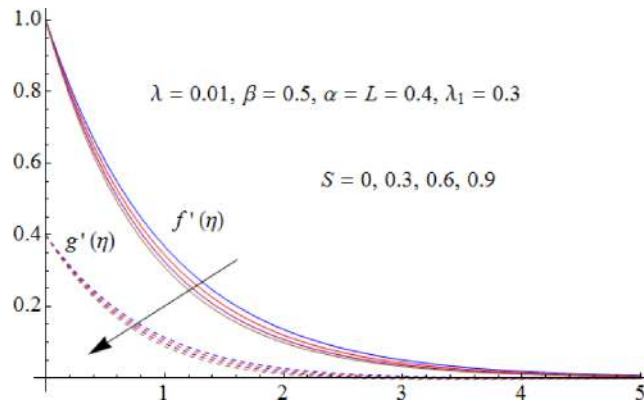FIG. 5. Behavior of α on $f'(\eta)$ and $g'(\eta)$.
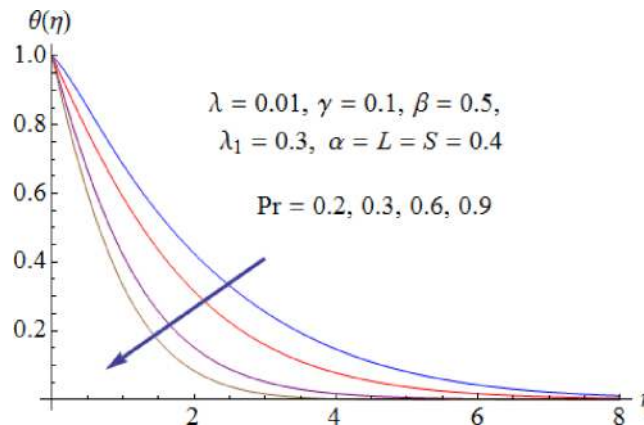

FIG. 6. Behavior of S on $f'(\eta)$ and $g'(\eta)$.

FIG. 7. Behavior of Pr on $\theta(\eta)$.

relaxation time on fluid temperature can be analyzed from Fig. 8. There is a decrease in temperature and thermal boundary layer thickness when γ enhances. This is due to the fact that as we increase γ particles show non-conducting behavior i.e. particles need more time to transfer heat to its neighboring particles as a result temperature decreases. Fig. 9 shows the influence of stretching rates ratio α on temperature profile. We observed that temperature decreases when α is increased because
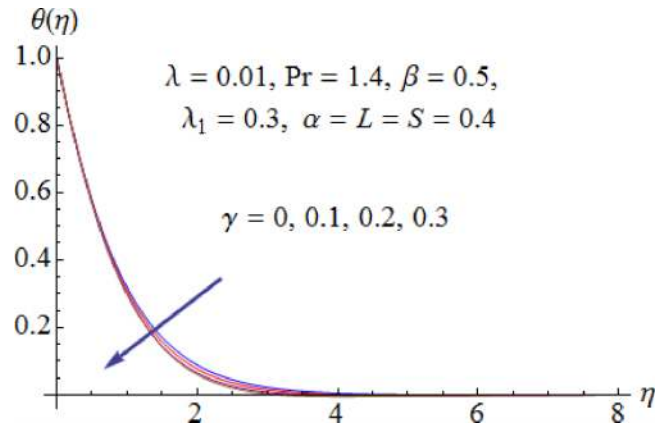
FIG. 8. Behavior of γ on $\theta(\eta)$.
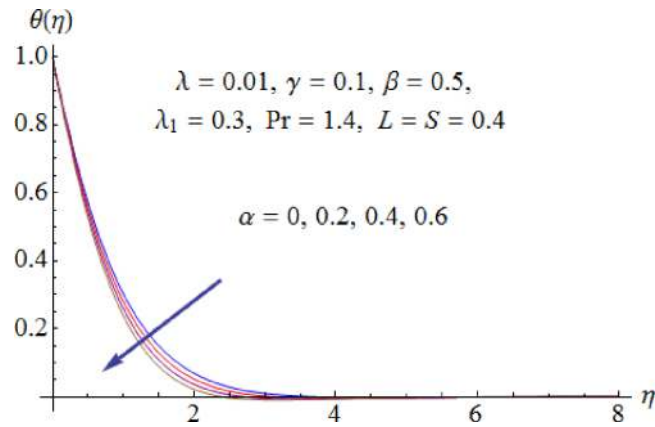
FIG. 9. Behavior of α on $\theta(\eta)$.
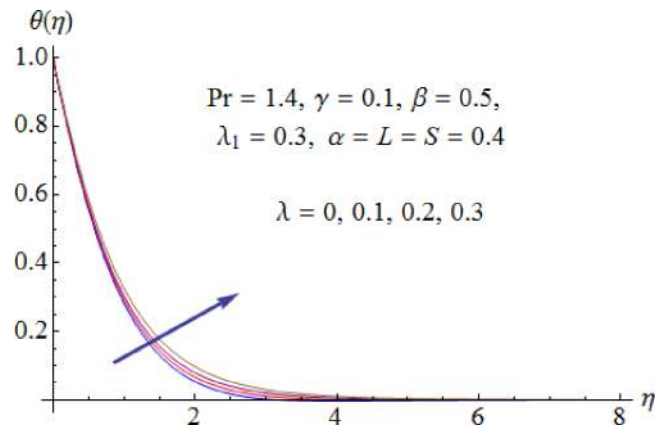
FIG. 10. Behavior of λ on $\theta(\eta)$.

for increasing α fluid velocity increases it means there is less resistance for fluid motion so less heat produces. Also Fig. 10 depicts that for higher value of rotational parameter λ the temperature profile $\theta(\eta)$ increases. For increasing values of λ_1 fluid velocity decrease which shows that there is more resistance for fluid flow as a result large amount of heat produces consequently temperature increases (see Fig. 11).
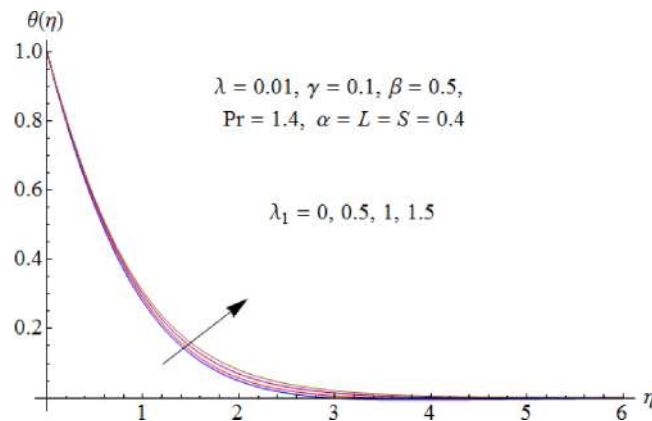
FIG. 11. Behavior of λ_1 on $\theta(\eta)$.

VI. CONCLUSIONS

Three dimensional flow of Jeffrey fluid by considering Cattaneo-Christov heat flux model over a porous stretching sheet is studied. Key points are summarized as follows:

- Velocity profiles f' and g' are decreasing functions of ratio of relaxation to retardation times and increasing function of Deborah number.
- Temperature profile decreases with the increase in Prandtl number and thermal relaxation time.
- Stretching rates ratio and rotational parameter have opposite impact on temperature profile.
- Influences of embedded parameters is found qualitatively similar in both Fourier and Cattaneo-Christov heat conduction models.

[1] J. B. J. Fourier, *Theorie analytique De La chaleur* (Paris, 1822).
[2] C. Cattaneo, "Sulla conduzione del calore," Atti Semin. Mat. Fis. Univ. Modena Reggio Emilia **3**, 83–101 (1948).
[3] C. I. Christov, "On frame indifferent formulation of the Maxwell-Cattaneo model of finite speed heat conduction," Mechanics Research Communications **36**, 481–486 (2009).
[4] V. Tibullo and V. Zampoli, "A uniqueness result for the Cattaneo–Christov heat conduction model applied to incompressible fluids," Mechanics Research Communications **38**, 77–79 (2011).
[5] B. Straughan, "Thermal convection with the Cattaneo-Christov model," International Journal of Heat and Mass Transfer **53**, 95–98 (2010).
[6] M. Ciarletta and B. Straughan, "Uniqueness and structural stability for the Cattaneo–Christov equations," Mechanics Research Communications **37**, 445–447 (2010).
[7] S. Han, L. Zheng, C. Li, and X. Zhang, "Coupled flow and heat transfer in viscoelastic fluid with Cattaneo–Christov heat flux model," Applied Mathematics Letters **38**, 87–93 (2014).
[8] M. Mustafa, "Cattaneo-Christov heat flux model for rotating flow and heat transfer of upper-convected Maxwell fluid," AIP Advances **5**, 047109 (2015).
[9] D. Tripathi, N. Ali, T. Hayat, M. K. Chaube, and A. A. Hendi, "Peristaltic flow of MHD Jeffrey fluid through a finite length cylindrical tube," Applied Mathematics and Mechanics (English Edition) **32**, 1148–1160 (2011).
[10] T. Hayat, S. A. Shehzad, M. Qasim, and S. Obaidat, "Radiative flow of Jeffery fluid in a porous medium with power law heat flux and heat source," Nuclear Engineering Design **243**, 15–19 (2012).
[11] M. Turkyilmazoglu and I. Pop, "Exact analytical solutions for the flow and heat transfer near the stagnation point on a stretching/shrinking sheet in a Jeffrey fluid," International Journal of Heat and Mass Transfer **57**, 82–88 (2013).
[12] S. A. Shehzad, A. Alsaedi, and T. Hayat, "Influence of thermophoresis and Joule heating on the radiative flow of Jeffrey fluid with mixed convection," Brazilian Journal of Chemical Engineering **30**, 897–908 (2013).
[13] K. Das, "Influence of slip and heat transfer on MHD peristaltic flow of a Jeffrey fluid in an inclined asymmetric porous channel," Indian Journal of Mathematics **54**(1), 19–45 (2012).
[14] G. B. Reddy, S. Sreenadh, R. H. Reddy, and A. Kavitha, "Flow of a Jeffrey fluid between torsionally oscillating disks," Ain Shams Engineering Journal **6**, 355–362 (2015).
[15] T. Hayat, S. A. Shehzad, and A. Alsaedi, "Three-dimensional stretched flow of Jeffery fluid with variable thermal conductivity and thermal radiation," Applied Mathematics and Mechanics (English Edition) **34**, 823–832 (2013).
[16] S. A. Shehzad, T. Hayat, A. Alsaedi, and M. A. Obid, "Nonlinear thermal radiation in three-dimensional flow of Jeffrey nanofluid: A model for solar energy," Applied Mathematics and Computation **248**, 273–286 (2014).
[17] L. J. Crane, "Flow past a stretching plate," Zeitschrift für angewandte Mathematik und Physik ZAMP **21**, 645–647 (1970).
[18] S. Abbasbandy, T. Hayat, A. Alsaedi, and M. M. Rashidi, "Numerical and analytical solutions for Falkner-Skan flow of MHD Oldroyd-B fluid," International Journal of Numerical Methods for Heat and Fluid Flow **24**, 390–401 (2014).

[19] W. Ibrahim, B. Shankar, and M. M. Nandeppanavar, "MHD stagnation point flow and heat transfer due to nanofluid towards a stretching sheet," International Journal of Heat and Mass Transfer **56**, 1–9 (2013).

[20] A. Malvandi, F. Hedayati, and D. D. Ganji, "Slip effects on unsteady stagnation point flow of a nanofluid over a stretching sheet," Powder Technology **253**, 377–384 (2014).

[21] P. D. Weidman and A. Ishak, "Multiple solutions of two-dimensional and three-dimensional flows induced by a stretching flat surface," Communications in Nonlinear Science and Numerical Simulation **25**, 1–9 (2015).

[22] T. Hayat, S. Asad, M. Mustafa, and A. Alsaedi, "Radiation effects on the flow of Powell-Eyring fluid past an unsteady inclined stretching sheet with non-uniform heat source/sink," Plos One **9**, e103214 (2014).

[23] Y. Lin, L. Zheng, and G. Chen, "Unsteady flow and heat transfer of pseudo-plastic nanoliquid in a finite thin film on a stretching surface with variable thermal conductivity and viscous dissipation," Powder Technology **274**, 324–332 (2015).

[24] J. Sui, L. Zheng, X. Zhang, and G. Chen, "Mixed convection heat transfer in power law fluids over a moving conveyor along an inclined plate," International Journal of Heat and Mass Transfer **85**, 1023–1033 (2015).

[25] M. M. Rashidi, M. Ali, N. Freidoonimehr, B. Rostami, and A. Hossian, "Mixed convection heat transfer for viscoelastic fluid flow over a porous wedge with thermal radiation," Advances in Mechanical Engineering **204**, 735939 (2014).

[26] U. Farooq, Y. L. Zhao, T. Hayat, A. Alsaedi, and S. J. Liao, "Application of the HAM-based mathematica package BVPh 2.0 on MHD Falkner-Skan flow of nanofluid," Computers & Fluids **111**, 69–75 (2015).

[27] S. Abbasbandy, M. Yurusoy, and H. Gulluce, "Analytical solutions of non-linear equations of power-law fluids of second grade over an infinite porous plate," Mathematical & Computational Applications **19**(2), 124 (2014).

[28] D. D. Ganji, M. Abbasi, J. Rahimi, M. Gholami, and I. Rahimipetroudi, "On the MHD squeeze flow between two parallel disks with suction or injection via HAM and HPM," Frontiers of Mechanical Engineering **9**, 270–280 (2014).

[29] T. Hayat, A. Shafiq, M. Mustafa, and A. Alsaedi, "Boundary-layer flow of Walters' B fluid with Newtonian heating," Zeitschrift fur Naturforschung A **70**(5), 333–341 (2015).

[30] T. Hayat, M. Imtiaz, and A. Alsaedi, "Impact of magnetohydrodynamics in bidirectional flow of nanofluid subject to second order slip velocity and homogeneous–heterogeneous reactions," Journal of Magnetism and Magnetic Materials **395**, 294–302 (2015).